Bremsstrahlung and Pair Production in the Field of Free Electrons

E. Haug

Lehrstuhl für Theoretische Astrophysik, Universität Tübingen

A formula is given for the doubly differential cross section of electron-electron bremsstrahlung which is exact in lowest-order perturbation theory. Angular distributions and energy spectra of the emitted photon are calculated in the center-of-mass system and the laboratory system. The cross section for pair production in the field of an electron (triplet production) can be derived from the analogous bremsstrahlung formula using the substitution rule. Angular distributions and energy spectra of the produced positron as well as the total cross section for triplet production are computed in the laboratory system. The results for bremsstrahlung and pair production are compared with previous theoretical calculations.

1. Introduction

The fully differential cross sections for pair production and bremsstrahlung in the field of unpolarized electrons were first calculated by Votruba[1] and Hodes[2], respectively, in lowest-order perturbation theory. Compared to the familiar Bethe-Heitler formulae[3] for the corresponding processes in the Coulomb field of a nucleus, these expressions are extremely complicated due to recoil and exchange effects[4]. Therefore the common practice was to use approximations, either by considering the nonrelativistic[5,6] and the high-energy[1,6-9] limits or by neglecting some of the eight Feynman diagrams contributing to the processes[10,11]. In the first case the cross sections for the intermediate region of energies had to be evaluated by interpolation, in the second case the importance of the missing terms was not well understood except for very high energies. In the last few years there were also efforts to use the exact formula for pair production with the aid of computers[12-14]. However, the numerical integrations of the differential cross section are quite cumbersome and expensive. Furthermore the errors are relatively large and the accuracy becomes poor at high energies.

In this paper a manageable formula for the cross section of bremsstrahlung in the field of an electron is given. It was obtained by integrating analytically the fully differential cross section over the angles of the outgoing electrons, without any approximations. Since the formula is expressed as a function of invariant products, it can be specialized to any frame of reference, e. g. the center-of-mass system or the

laboratory system. The cross sections differential with respect to the photon energy can easily be computed by a single numerical integration. The results are used to determine the accuracy of the various approximations.

The differential cross section for pair production can be derived from the corresponding bremsstrahlung formula by applying the well-known substitution law[4,15]. By performing two numerical integrations, the total cross section has been computed with high accuracy. It is compared with the results of previous papers.

Screening and atomic binding of the electrons is not taken into account throughout this paper.

2. Bremsstrahlung Cross Section

In the elementary process of electron-electron bremsstrahlung (Fig. 1) two electrons with the four-momenta $\mathbf{p}_1 = (\varepsilon_1, \boldsymbol{p}_1)$ and $\mathbf{p}_2 = (\varepsilon_2, \boldsymbol{p}_2)$ are colliding under the emission of a photon with the four-momentum $\mathbf{k} = (k, \boldsymbol{k})$[16]. The outgoing electrons have the four-momenta $\mathbf{p}_1' = (\varepsilon_1', \boldsymbol{p}_1')$ and $\mathbf{p}_2' = (\varepsilon_2', \boldsymbol{p}_2')$. The differential cross section for unpolar-
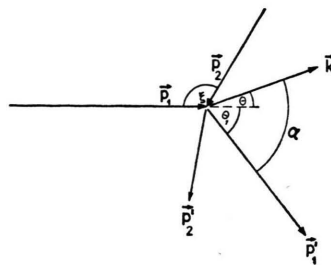

Fig. 1. Elementary process of electron-electron bremsstrahlung.

ized particles is given by [4]

$$d\sigma = \frac{a\,r_0^2}{\pi^2}\,\frac{\delta^{(4)}(\mathbf{p}_1+\mathbf{p}_2-\mathbf{p}_1{}'-\mathbf{p}_2{}'-\mathbf{k})}{V(p_1\,p_2)^2-1}$$
$$\cdot A\,\frac{d^3p_1{}'}{\varepsilon_1{}'}\,\frac{d^3p_2{}'}{\varepsilon_2{}'}\,\frac{d^3k}{k}\qquad(2.1)$$

where $a\approx\frac{1}{137}$, $r_0=e^2/m\,c^2$, and A is a function of invariant products between the four-momenta of the particles. By squaring the conservation law

$$\mathbf{p}_1+\mathbf{p}_2=\mathbf{p}_1{}'+\mathbf{p}_2{}'+\mathbf{k}\qquad(2.2)$$

the relation

$$(p_1\,p_2)=(p_1{}'\,p_2{}')+(k\,p_1)+(k\,p_2)\qquad(2.3)$$

can be derived. With the Eqs. (2.2) and (2.3) only 5 of the 10 possible invariant products are independent.

The complicated function A was obtained by using the traces evaluated by Anders [17]. Because the expression for A is very lengthy, it is not given here. A comparison of the resulting cross sections with those computed by Mack and Mitter [18] yielded excellent agreement so that the correctness of the function A is guaranteed. The integration of (2.1) over $d^3p_2{}'$ is easily performed using

$$\delta^{(3)}(\mathbf{p}_1+\mathbf{p}_2-\mathbf{p}_1{}'-\mathbf{p}_2{}'-\mathbf{k})\,.$$

With the aid of the relations

$$d^3p_1{}'=p_1{}'^2\,dp_1{}'\,d\Omega_{p_1'}\qquad(2.4)$$
$$=\varepsilon_1{}'\,p_1{}'\,d\varepsilon_1{}'\,d\Omega_{p_1'},\ d^3k=k^2\,dk\,d\Omega_k$$

and

$$\delta(\varepsilon_1+\varepsilon_2-\varepsilon_1{}'-\varepsilon_2{}'-k)\,d\varepsilon_1{}'$$
$$=\frac{\varepsilon_2{}'\,p_1{}'^2}{|\,\varepsilon_2{}'\,p_1{}'^2-\varepsilon_1{}'(\mathbf{p}_1{}'\cdot\mathbf{p}_2{}')\,|}=\frac{\varepsilon_2{}'\,p_1{}'}{W}\qquad(2.5)$$

where

$$\varepsilon_2{}'=V(\mathbf{p}_1+\mathbf{p}_2-\mathbf{p}_1{}'-\mathbf{k})^2+1\qquad(2.6)$$

and

$$W=V[\,(p_1{}'\,p_2{}')+1\,]^2+[\mathbf{p}_1{}'\cdot(\mathbf{p}_1+\mathbf{p}_2-\mathbf{k})\,]^2/p_1{}'^2-(\varepsilon_1+\varepsilon_2-k)^2,\qquad(2.7)$$

the fully differential cross section becomes

$$\frac{d^3\sigma}{dk\,d\Omega_k\,d\Omega_{p_1'}}=\frac{a\,r_0^2}{\pi^2}\,\frac{k\,p_1{}'^2}{V(p_1\,p_2)^2-1}\,\frac{A}{W}\,.\qquad(2.8)$$

The momentum $p_1{}'=|\mathbf{p}_1{}'|$ of the outgoing electron as expressed by the vectors $\mathbf{p}_1$, $\mathbf{p}_2$ and $\mathbf{k}$ has the form

$$p_1{}'=\frac{[\,(p_1{}'\,p_2{}')+1\,]\,\mathbf{p}_1{}'\cdot(\mathbf{p}_1+\mathbf{p}_2-\mathbf{k})/p_1{}'\pm(\varepsilon_1+\varepsilon_2-k)\,W}{(\varepsilon_1+\varepsilon_2-k)^2-[\mathbf{p}_1{}'\cdot(\mathbf{p}_1+\mathbf{p}_2-\mathbf{k})\,]^2/p_1{}'^2}\,.\qquad(2.9)$$

The choice of the signs in the numerator depends on the frame of reference considered. The product $(p_1{}'\,p_2{}')$ occurring in (2.7) and (2.9) can be substituted by means of Equation (2.3).

It is easy to be seen that the function W takes a very simple shape if one specializes to the center-of-mass system S′ of the outgoing electrons, where

$$\mathbf{p}_1{}'+\mathbf{p}_2{}'=\mathbf{p}_1+\mathbf{p}_2-\mathbf{k}=0,\qquad(2.10)$$
$$\varepsilon_1{}'=\varepsilon_2{}'=\tfrac{1}{2}(\varepsilon_1+\varepsilon_2-k),\quad(p_1{}'\,p_2{}')=2\,\varepsilon_1{}'^2-1\,.$$

Then

$$W_{\mathrm{S}'}=2\,\varepsilon_1{}'\,p_1{}'\qquad(2.11)$$

and the cross section is given by

$$\left(\frac{d^3\sigma}{dk\,d\Omega_k\,d\Omega_{p_1'}}\right)_{\mathrm{S}'}=\frac{a\,r_0^2}{2\,\pi^2}\,\frac{k\,p_1{}'}{\varepsilon_1{}'}\,\frac{A}{V(p_1\,p_2)^2-1}\,.\qquad(2.12)$$

This equation is the most convenient starting point for the integration over the solid angle $\Omega_{p_1'}$ since only the function A is dependent on the angles of the final electrons, and this expression can be integrated exactly. As the momenta $\mathbf{p}_1$, $\mathbf{p}_2$ and $\mathbf{k}$ form a triangle in the system S′ [cf. Eq. (2.10)], the orientation of the vectors $\mathbf{p}_1{}'$ and $\mathbf{p}_2{}'=-\mathbf{p}_1{}'$ is quite arbitrary. So the full solid angle $\Omega_{p_1'}=4\,\pi$ is possible kinematically, i. e., the limits of integration are independent of $\mathbf{p}_1$, $\mathbf{p}_2$, and $\mathbf{k}$. After having carried out the integrations, the result has to be divided by 2 since any final state of the identical particles occurs twice.

The laborious but elementary integration yields a cross section which again can be expressed in covariant form, namely by the 3 invariant products $(p_1\,p_2)$, $(k\,p_1)$ and $(k\,p_2)$. Hence it is valid in any frame of reference.

Using the notations

$$w^2=(\mathbf{p}_1+\mathbf{p}_2)^2=2\,[\,(p_1\,p_2)+1\,]\qquad(2.13)$$

and

$$\varrho^2 = (\mathbf{p_1}' + \mathbf{p_2}')^2 = 2\left[(p_1' p_2') + 1\right]$$
$$= 2\left[(p_1 p_2) - (k p_1) - (k p_2) + 1\right] \qquad (2.14)$$

the bremsstrahlung cross section differential with respect to the photon energy and photon angles can be written as

$$\sigma(k,\theta) \equiv \frac{\mathrm{d}^2\sigma}{\mathrm{d}k\,\mathrm{d}\Omega_k}$$
$$= \frac{\alpha\, r_0^2}{\pi} \frac{k}{w\,\varrho} \sqrt{\frac{\varrho^2 - 4}{w^2 - 4}} \frac{1}{\pi} \int A\,\mathrm{d}\Omega_{p_1'}. \qquad (2.15)$$

The expression for $1/\pi \int A\,\mathrm{d}\Omega_{p_1'}$ is given in the Appendix. It is not possible to integrate $\mathrm{d}^2\sigma/\mathrm{d}k\,\mathrm{d}\Omega_k$ over the photon angles analytically. However, the numerical computation of the cross section

$$\sigma(k) \equiv \frac{\mathrm{d}\sigma}{\mathrm{d}k} = \int \frac{\mathrm{d}^2\sigma}{\mathrm{d}k\,\mathrm{d}\Omega_k}\mathrm{d}\Omega_k \qquad (2.16)$$

is quite easy in the center-of-mass system and in the laboratory system where one of the electrons is initially at rest: Because of the rotational symmetry around the momentum vector $\mathbf{p_1}$ the cross section $\sigma(k,\theta)$ is not dependent on the azimuthal angle; so the solid angle of the outgoing photon is simply given by

$$\mathrm{d}\Omega_k = 2\,\pi \sin\theta\,\mathrm{d}\theta \qquad (2.17)$$

and one has to perform only one single integration over the angle θ between $\mathbf{p_1}$ and $\mathbf{k}$.

In the general case of arbitrary directions of the momenta $\mathbf{p_1}$ and $\mathbf{p_2}$ the computation of $\sigma(k)$ needs two integrations.

3. Coulomb Correction

The cross-section formulae derived in the preceding section are exact within lowest-order perturbation theory. Whereas radiative corrections are assumed to be small, the Coulomb correction may be important for low energies. Correct results can be expected only if the conditions

$$a_1 = \alpha/\beta_{12} \ll 1, \quad a_2 = \alpha/\beta'_{12} \ll 1 \qquad (3.1)$$

are satisfied, where

$$\beta_{12} = \frac{\sqrt{(p_1 p_2)^2 - 1}}{(p_1 p_2)} = \frac{w\sqrt{w^2 - 4}}{w^2 - 2} \qquad (3.2)$$

and

$$\beta'_{12} = \frac{\sqrt{(p_1' p_2')^2 - 1}}{(p_1' p_2')} = \frac{\varrho\sqrt{\varrho^2 - 4}}{\varrho^2 - 2} \qquad (3.3)$$

are the relative velocities of the initial and final electrons, respectively, in units of the speed of light, c. For the bremsstrahlung process in the field of a nucleus, the cross section in Born approximation can be corrected by a simple factor derived by Elwert [19] for nonrelativistic energies. This factor which is given by the ratio of probabilities for finding the final and initial electron, respectively, at the position of the nucleus, has been shown [20] to yield correct results in the full energy region for nuclei with low atomic numbers Z. In case of electron-electron bremsstrahlung a corresponding correction factor can be found by calculating the ratio of probabilities of finding the two initial and final electrons, respectively, at the same position. It has the form [21]

$$F_{ee} = \frac{a_2}{a_1} \frac{e^{2\pi a_1} - 1}{e^{2\pi a_2} - 1}. \qquad (3.4)$$

In contrast to the electron-nucleus case, this factor is always less than unity, as a consequence of the Coulomb repulsion between the electrons. That is, the true cross section is always lower than the one given by the formulae of Section 2. Due to the small factor $\alpha \approx \frac{1}{137}$ in the quantities a_1 and a_2, however, F_{ee} is approximately unity, especially for higher energies. An important exception is the short-wavelength limit given by $\varrho \to 2$. Then $a_2 \to \infty$ and $F_{ee} \to 0$. As can be seen from Eqs. (2.15) and (A1), $\sigma(k,\theta)$ tends to zero for $\varrho \to 2$. This behaviour is still intensified by the Coulomb correction. Thus the true cross section at the high-frequency limit is equal to zero whereas the short-wavelength cross section of the electron-nucleus bremsstrahlung becomes finite by applying the Elwert factor, as is well known.

Generally, the factor (3.4) is dependent on the momenta $\mathbf{p_1}$, $\mathbf{p_2}$ and $\mathbf{k}$, i.e., it is different for various photon angles. In the center-of-mass system, however, $\varrho^2 = 4\,\varepsilon_1(\varepsilon_1 - k)$ so that F_{ee} is constant for a given photon energy k.

In the following sections the Coulomb factor is not taken into account because its effect is not significant at the energies considered.

4. Differential Cross Sections for Electron-Electron Bremsstrahlung: Results

The formula (A1) can easily be programmed for the computation of the doubly differential cross

section $\sigma(k,\theta)$. One should, however, pay attention to the fact that a high accuracy is needed in order to prevent round-off errors. The real variables of the CDC-3300 computer used have 11 decimal digits which frequently were not sufficient, especially in calculating cross sections for low photon energies k and small photon angles θ. In these cases numbers with double precision had to be employed. Otherwise the computation of $\sigma(k,\theta)$ is straightforward.

4.1. Center-of-Mass System

The center-of-mass system (cms) is defined by

$$\boldsymbol{p}_1 + \boldsymbol{p}_2 = \boldsymbol{p}_1' + \boldsymbol{p}_2' + \boldsymbol{k} = 0. \qquad (4.1.1)$$

With that the invariants w^2 and ϱ^2 reduce to

$$w^2 = 4\,\varepsilon_1{}^2, \quad \varrho^2 = 4\,\varepsilon_1(\varepsilon_1 - k), \qquad (4.1.2)$$

i. e., they are independent of angles. Because of the symmetry of Eq. (A1) with respect to the products

$$x_1 = (k\,p_1) = k(\varepsilon_1 - p_1 \cos\theta),$$
$$x_2 = (k\,p_2) = k(\varepsilon_1 + p_1 \cos\theta) \qquad (4.1.3)$$

where θ is the photon angle relative to $\boldsymbol{p}_1$, the photon distributions in the cms are symmetric to $\theta = \pi/2$, and all angles θ are allowed kinematically.

Figure 2 shows the cross section $\sigma(k,\theta)$ as a function of θ for the kinetic energy $E_1 = E_2 = (\varepsilon_1 - 1)\,m\,c^2 = 300\,\text{keV}$ of the initial electrons and for various photon energies $h\,\nu = m\,c^2\,k$. As expected most of the photons are emitted near $\theta = 0$ and $\theta = \pi$. This feature is more pronounced at higher energies (Fig. 3) where the width of the curves at half maximum is $\theta_{1/2} \approx 1/2\,\varepsilon_1$. Around $\theta = \pi/2$ the cross section has decreased by several orders of magnitude.

An excellent approximation for the bremsstrahlung cross section in the cms at extreme relativistic energies has been given by Baier, Fadin and Khoze [9]
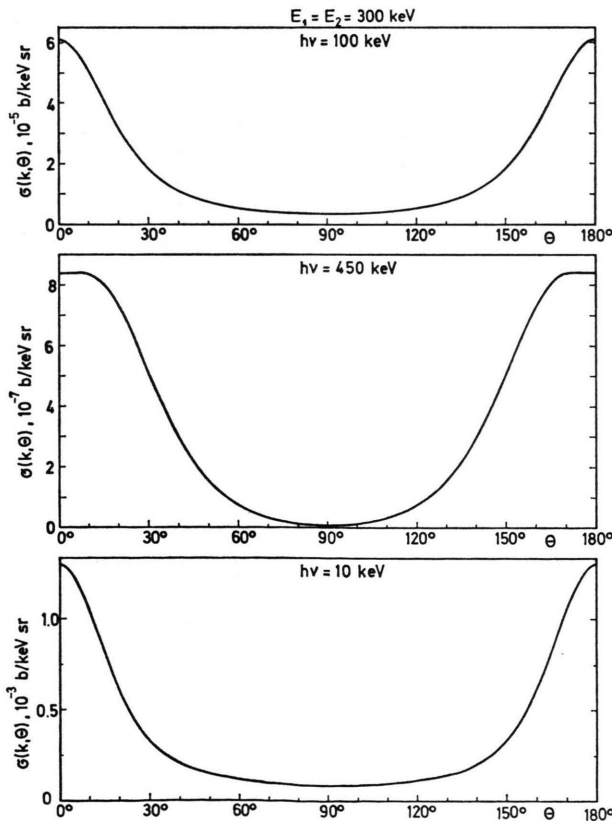
Fig. 2. Cross section $\sigma(k,\theta)$ of electron-electron bremsstrahlung in the cms for the kinetic electron energies $E_1 = E_2 = 300\,\text{keV}$ and various photon energies $h\,\nu$.

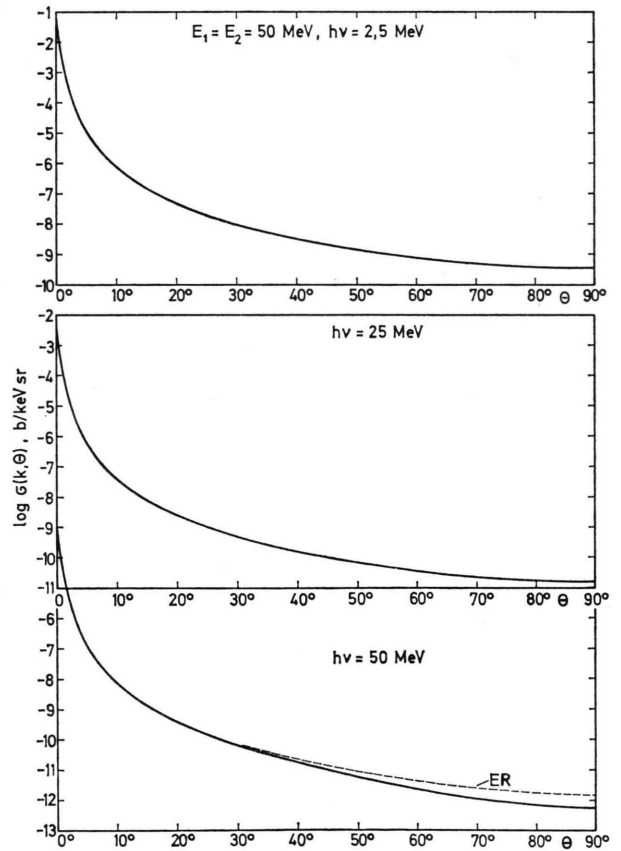Fig. 3. Cross section $\sigma(k,\theta)$ of electron-electron bremsstrahlung in the cms for $E_1 = E_2 = 50\,\text{MeV}$ and various photon energies $h\,\nu$. The broken line labelled ER represents the extreme relativistic approximation of BFK [9].

(BFK) who systematically expanded all quantities in powers of $1/\varepsilon_1^2$ and retained only the leading terms of the expansion. The agreement between the BFK formula [22] and the results of this paper is better than 0.1% for $E_1 = E_2 = 50$ MeV and the important photon angles. The only distinct differences appear very close to the high-frequency limit $k = p_1^2/\varepsilon_1$ at large angles θ (Figure 3). This is not significant because the cross section is very low there.

4.2. Laboratory System

In the laboratory system one of the initial electrons is at rest. For $\boldsymbol{p}_2 = 0$ the quantities w^2 and ϱ^2 have the form

$$w^2 = 2(\varepsilon_1 + 1), \quad \varrho^2 = 2[\varepsilon_1 + 1 - k(\varepsilon_1 + 1 - p_1 \cos \theta)]. \tag{4.2.1}$$

The maximum photon energy occurs for $\varrho^2 = 4$ and is given by

$$k_{\max}(\varepsilon_1, \theta) = (\varepsilon_1 - 1)/(\varepsilon_1 + 1 - p_1 \cos \theta). \tag{4.2.2}$$

The absolute maximum of k is in forward direction $\theta = 0$:

$$k_{\max}(\varepsilon_1) = (\varepsilon_1 - 1)/(\varepsilon_1 - p_1 + 1) \tag{4.2.3}$$

A photon with $(\varepsilon_1 - 1)/(\varepsilon_1 + p_1 + 1) < k \leq k_{\max}(\varepsilon_1)$ can be emitted only into a cone with the half apex angle θ_0 given by

$$\cos \theta_0 = [(\varepsilon_1 + 1) k - (\varepsilon_1 - 1)]/k p_1. \tag{4.2.4}$$

As k increases, the allowed angular region is more and more limited as can be seen in Figure 4.

For extreme relativistic energies the electron-electron bremsstrahlung is emitted essentially into a narrow cone in forward direction (Figure 5). The angle of half maximum is about $1/2 \varepsilon_1$, the same value as in the electron-nucleus case. The formula derived by Baier, Fadin and Khoze [8] for high-energy electrons is a good approximation for small angles θ and sufficiently far away from the short-

Fig. 4. Cross section $\sigma(k, \theta)$ of electron-electron bremsstrahlung in the laboratory system for the kinetic electron energy $E_1 = 300$ keV and various photon energies $h\nu$.
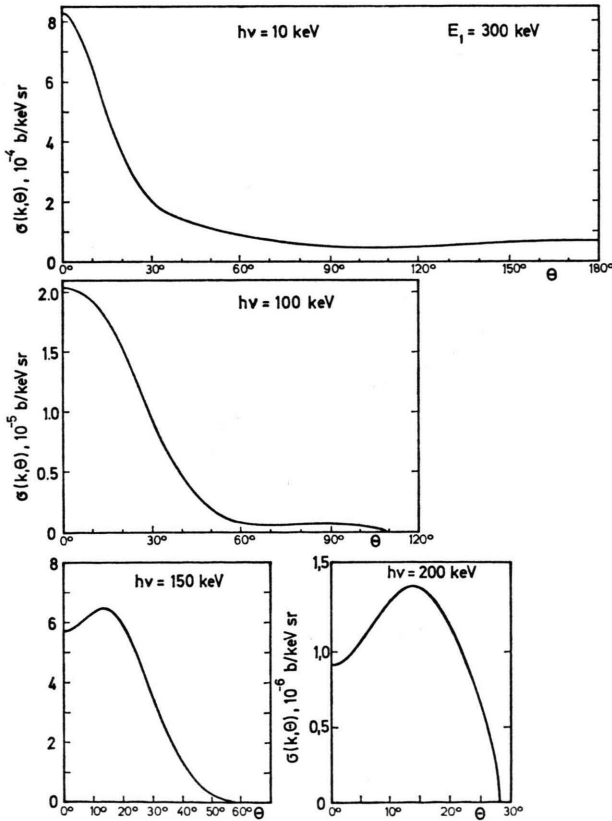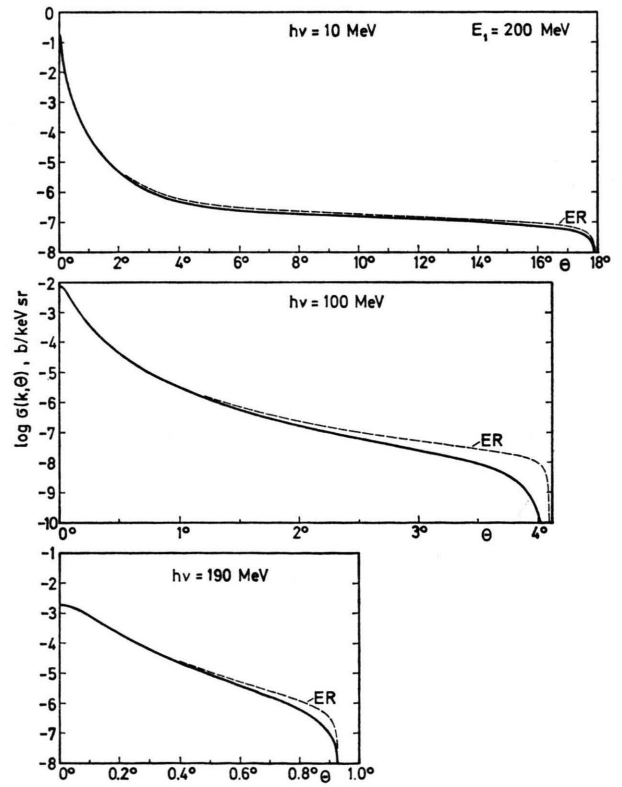

Fig. 5. Cross section $\sigma(k, \theta)$ of electron-electron bremsstrahlung in the laboratory system for $E_1 = 200$ MeV and various photon energies $h\nu$. The broken lines labelled ER show the extreme relativistic approximation of BFK [8].

wavelength limit, where $\varepsilon_1 - k = 0(1)$. Near the limiting angle θ_0 the results are the poorer the higher the photon energy is (Figure 5). There are two reasons why this approximation formula does not compare as favourably with the exact results as in case of the cms: (1) The reciprocal expansion parameter $(p_1 p_2)$ is equal to ε_1 in the lab system, but it is proportional to the square of ε_1 in the cms. (2) Whereas the expression [9] in the cms is valid for the whole bremsstrahlung spectrum, the cross section of Ref. [8] was obtained under the assumption that $\varepsilon_1 - k \gg 1$. A formula corresponding to the one in the cms is not available in the lab system.

Since the momentum transfer to the recoiling electron is very low at the important angles $\theta \lesssim 1/\varepsilon_1$, the nuclear cross section for unit charge may also be applied to the electron-electron process with satisfactory accuracy [4].

5.1. The Photon Spectrum in the Center-of-Mass System

The photon spectra are calculated by numerical integration of the angular distributions $\sigma(k, \theta)$ in the cms.

Fedyushin [5] and Garibyan [6, 23] have derived the cross section for electron-electron bremsstrahlung in nonrelativistic approximation which can be written as

$$\frac{d\sigma_{NR}}{dk} = \frac{4}{15} \frac{\alpha r_0^2}{k} F\left(\frac{k}{p_1^2}\right) \quad (5.1.1)$$

where

$$F(x) = \left[17 - \frac{3x^2}{(2-x)^2}\right] \sqrt{1-x}\cdot$$
$$+ \frac{12(2-x)^4 - 7x^2(2-x)^2 - 3x^4}{(2-x)^3} \ln \frac{1+\sqrt{1-x}}{\sqrt{x}}. \quad (5.1.2)$$

This expression agrees quite well with the exact cross section for kinetic electron energies below $E_1 = E_2 \approx 10$ keV; then the error is of the order of a few percent. In the region of intermediate energies, however, Eq. (5.1.1) may be used only as a rough estimate of the true values, as is seen in Figure 6. If $\varepsilon_1 - 1 \ll 1$ is no more valid, the argument of the function F has to be replaced by $k/k_{max} = \varepsilon_1 k/p_1^2$ in order that $d\sigma_{NR}/dk$ may vanish at the short-wavelength limit.
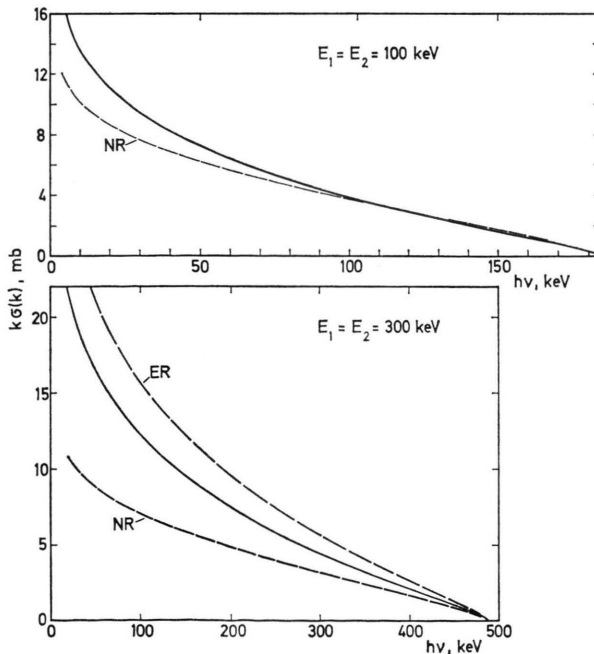

Fig. 6. Electron-electron bremsstrahlung in the cms: photon spectra for the kinetic electron energies $E_1 = E_2 = 100$ keV and 300 keV. The broken lines labelled NR and ER show the nonrelativistic and extreme relativistic approximations, respectively.
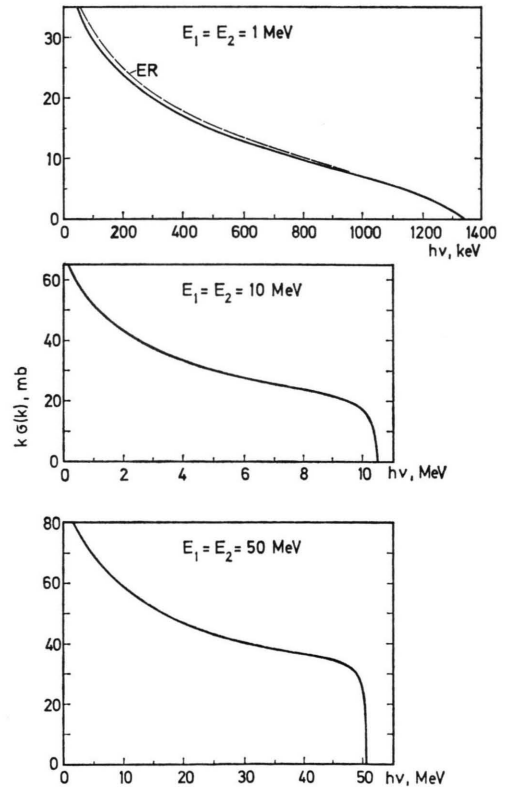
Fig. 7. Electron-electron bremsstrahlung in the cms: photon spectra for $E_1 = E_2 = 1$ MeV, 10 MeV, and 50 MeV. The broken line labelled ER shows the extreme relativistic approximation of BFK [9].

For the high-energy region Baier, Fadin and Khoze [9] have given a formula [24] which is valid for all photon energies including the hard end of the spectrum. As the corresponding expression for the differential cross section $\sigma(k, \theta)$ this is also an excellent approximation. In Fig. 7 is shown that the BFK formula is in good agreement with the exact one down to $E_1 = 1$ MeV. For $E_1 = 5$ MeV the error is less than 0.3% throughout and even for $E_1 = 300$ keV the BFK approximation is better than the nonrelativistic one (Figure 6). At very high energies there is a sharp drop of the cross section near the short-wavelength limit (Figure 7). This behaviour is also described precisely by the BFK formula, in contrast to the usual relativistic expression [8]

$$\frac{d\sigma_R}{dk} \approx \frac{8\,a\,r_0{}^2}{\varepsilon_1\,k}\left[\frac{4}{3}\,(\varepsilon_1-k) + \frac{k^2}{\varepsilon_1}\right]$$
$$\cdot\left[\ln\frac{4\,\varepsilon_1{}^2}{k}\,(\varepsilon_1-k) - \frac{1}{2}\right]. \quad (5.1.3)$$

As long as the photon energy is not very close to its maximum $k_{\max} = p_1{}^2/\varepsilon_1$, Eq. (5.1.3) is a good approximation for the cross section of electron-electron as well as of electron-positron [25] bremsstrahlung in the extreme relativistic case.

5.2. The Photon Spectrum in the Laboratory System

Figure 8 shows in a logarithmic scale the normalized cross section

$$\Phi(\varepsilon_1, k) = \frac{1}{a\,r_0{}^2}\,\frac{d\sigma}{dk} \quad (5.2.1)$$

as a function of the photon energy k for various kinetic electron energies E_1. Contrary to the electron-nucleus case these curves are not intersecting at low photon energies. This is due to the fact that the cross section for the electron-electron quadrupole radiation is small compared to the dipole emission of the electron-nucleus system. Sufficiently far away from the short-wavelength limit the curves are nearly straight lines in the logarithmic representation; the slope is about -1.1 to -1.2.

For the low-energy region a general formula can be derived from Eq. (5.1.1) taking into account that $\sigma_{NR}(k)$ has to be dependent on $|\boldsymbol{p}_1 - \boldsymbol{p}_2|$. The argument of F in (5.1.1) is equal to $k/k_{\max}$. If the momenta $\boldsymbol{p}_1$ and $\boldsymbol{p}_2$ of the initial electrons are arbitrary, the highest possible photon energy is [26]

$$k_{\max}(\boldsymbol{p}_1, \boldsymbol{p}_2) = \frac{(p_1\,p_2)-1}{\varepsilon_1 + \varepsilon_2 - |\boldsymbol{p}_1 + \boldsymbol{p}_2|}. \quad (5.2.2)$$

In the nonrelativistic limit this expression reduces to $k_{\max}(\boldsymbol{p}_1, \boldsymbol{p}_2) \approx \frac{1}{4}(\boldsymbol{p}_1 - \boldsymbol{p}_2)^2$. It is a function of $|\boldsymbol{p}_1 - \boldsymbol{p}_2|$; therefore in any frame of reference the nonrelativistic cross section can be written as

$$\frac{d\sigma_{NR}}{dk} = \frac{4}{15}\,\frac{a\,r_0{}^2}{k}\,F\left(\frac{4\,k}{[\boldsymbol{p}_1 - \boldsymbol{p}_2]^2}\right) \quad (5.2.3)$$

where $F(x)$ is given by (5.1.2). In the cms, this is equivalent to Eq. (5.1.1), and in the laboratory system

$$\left(\frac{d\sigma_{NR}}{dk}\right)_L = \frac{4}{15}\,\frac{a\,r_0{}^2}{k}\,F\left(\frac{4\,k}{p_1{}^2}\right). \quad (5.2.4)$$

Except for the neighborhood of the short-wavelength limit this formula describes quite well the photon spectrum for electron energies below $E_1 \approx 20$ keV.

For intermediate energies above $E_1 \approx 100$ keV Eq. (5.2.4) becomes more and more unsuitable (Figure 9). It may be improved a bit by replacing
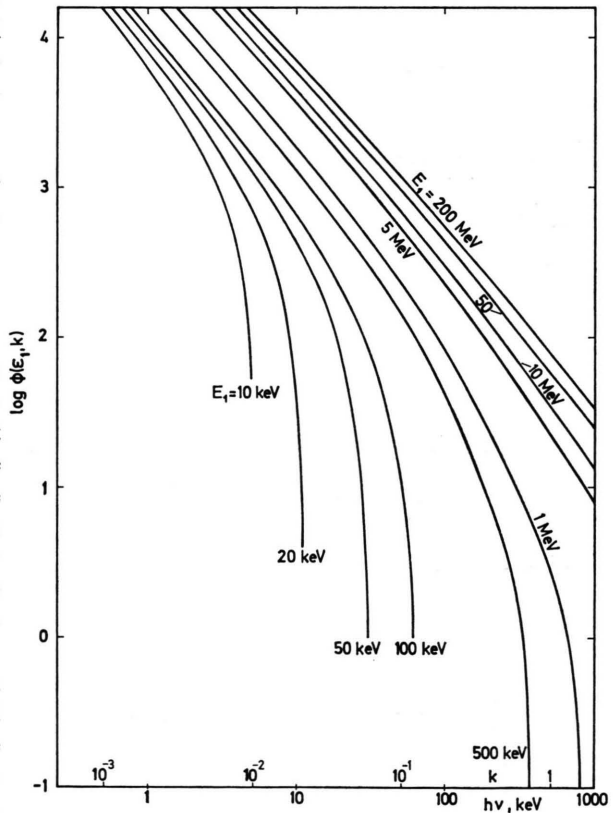

Fig. 8. Normalized cross section of electron-electron bremsstrahlung in the laboratory system as a function of the photon energy. The parameter is the kinetic energy of the incident electron, E_1.
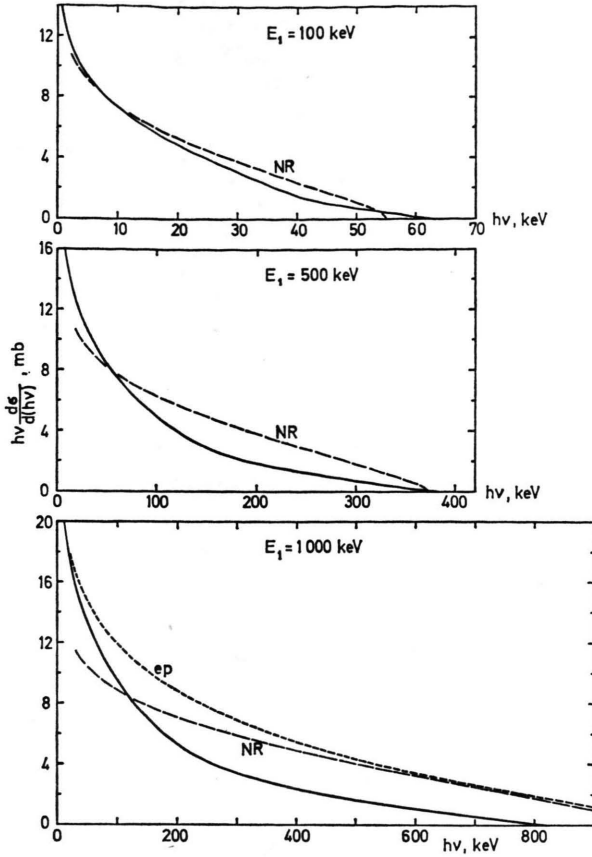
Fig. 9. Electron-electron bremsstrahlung in the laboratory system: photon spectra for the kinetic electron energies E_1 =100 keV, 500 keV, and 1000 keV compared to the cross section in nonrelativistic approximation (NR) and of electron-proton bremsstrahlung (ep).

Fig. 10. Electron-electron bremsstrahlung in the laboratory system: photon spectra for $E_1 = 5$ MeV, 50 MeV, and 1000 MeV. The broken lines labelled ER show the extreme relativistic approximation of BFK [8].

the argument of F by the exact value $k/k_{\max} = (\varepsilon_1 - p_1 + 1)k/(\varepsilon_1 - 1)$. However, this form yields worse results at low energies.

In the high-energy region the exact cross section may be compared with the formula of Baier, Fadin and Khoze [8]. As Fig. 10 shows, this approximation is not as good as the one in the cms. Even for electron energies E_1 which are hundred times the rest energy, the errors exceed 5% nearly in the whole spectrum. Only at $E_1 = 1000$ MeV the agreement is better than 1% apart from the vicinity of the high-frequency limit.

6. Cross Section for Pair Production

According to the substitution law [4, 15], the cross section for pair production in the field of an electron ("triplet production") can be derived from the

cross section for electron-electron bremsstrahlung. It requires a substitution for the four-momenta $\mathbf{p}_1$, $\mathbf{p}_2$, $\mathbf{p}_1'$, and $\mathbf{p}_2'$ of the initial and final electrons by the four-momenta $\mathbf{p}$, $\mathbf{p}'$, $-\mathbf{p}_+$, and $\mathbf{p}''$ of the initial and final electron and of the produced pair. The previously outgoing photon $-\mathbf{k}$ now becomes an incident photon $\mathbf{k}$. Taking into account that the flux density of the incoming particles is proportional to $(pk)/\varepsilon k$, the cross section (2.1) takes the form

$$d\sigma = \frac{\alpha r_0^2}{\pi^2} \frac{\delta^{(4)}(\mathbf{p} + \mathbf{k} - \mathbf{p}' - \mathbf{p}'' - \mathbf{p}_+)}{(pk)}$$
$$\cdot A_t \frac{d^3 p'}{\varepsilon'} \cdot \frac{d^3 p''}{\varepsilon''} \frac{d^3 p_+}{\varepsilon_+} \quad (6.1)$$

where the function A_t is connected with the corresponding expression A of the bremsstrahlung process by the above substitutions. Proceeding as in

Sect. 2, one obtains the fully differential cross section for unpolarized particles

$$\frac{d^3\sigma}{d\varepsilon_+ \, d\Omega_{p+} \, d\Omega_{p'}} = \frac{a \, r_0^2}{\pi^2} \frac{p'^2 \, p_+}{(p \, k)} \frac{A_t}{W_t} \, . \quad (6.2)$$

Here, $\mathbf{p}_+ = (\varepsilon_+, \boldsymbol{p}_+)$ is the four-momentum of the produced positron, $d\Omega_{p_+}$ and $d\Omega_{p'}$ are the solid angles into which the outgoing positron and one of the electrons emerge,

$$W_t = \sqrt{[(p' \, p'') + 1]^2 + [\boldsymbol{p}' \cdot (\boldsymbol{p} + \boldsymbol{k} - \boldsymbol{p}_+)]^2 / p'^2 - (\varepsilon + k - \varepsilon_+)^2} \quad (6.3)$$

and

$$p' = \frac{[(p' \, p'') + 1] [\boldsymbol{p}' \cdot (\boldsymbol{p} + \boldsymbol{k} - \boldsymbol{p}_+)]/ p' \pm (\varepsilon + k - \varepsilon_+) \, W_t}{(\varepsilon + k - \varepsilon_+)^2 - [\boldsymbol{p}' \cdot (\boldsymbol{p} + \boldsymbol{k} - \boldsymbol{p}_+)]^2 / p'^2} \, . \quad (6.4)$$

Corresponding to Eq. (2.3) the product $(p' \, p'')$ is given by

$$(p' \, p'') = (p \, k) - (p_+ \, k) - (p \, p_+) \, . \quad (6.5)$$

Again the function W_t takes the most simple form in the center-of-mass system S'' of the two outgoing electrons, where

$$\boldsymbol{p}' + \boldsymbol{p}'' = \boldsymbol{p} + \boldsymbol{k} - \boldsymbol{p}_+ = 0 \, . \quad (6.6)$$

Then

$$W_{S''} = 2 \, \varepsilon' \, p' \quad (6.7)$$

and

$$\left(\frac{d^3\sigma}{d\varepsilon_+ \, d\Omega_{p+} \, d\Omega_{p'}} \right)_{S''} = \frac{a \, r_0^2}{2 \, \pi^2} \frac{p' \, p_+}{\varepsilon'} \frac{A_t}{(p \, k)} \, . \quad (6.8)$$

This equation can be integrated exactly over the angles of the outgoing electron analogous to the case of electron-electron bremsstrahlung. The result is the cross section differential with respect to the energy and angles of the positron, valid in any frame of reference:

$$\frac{d^2\sigma}{d\varepsilon_+ \, d\Omega_{p+}} = \frac{a \, r_0^2}{2 \, \pi} \frac{p_+}{(p \, k)} \frac{\sqrt{\varrho_t^2 - 4}}{\varrho_t} \frac{1}{\pi} \int A_t \, d\Omega_{p'} \, . \quad (6.9)$$

Here

$$\varrho_t^2 = (\boldsymbol{p}' + \boldsymbol{p}'')^2 = 2 \, [(p' \, p'') + 1]$$
$$= 2 \, [(p \, k) - (p_+ \, k) - (p \, p_+) + 1] \, . \quad (6.10)$$

The integral $1/\pi \int A_t \, d\Omega_{p'}$ is given by Eq. (A1) with the substitutions $\varrho \to \varrho_t$, $w \to w_t$, $x_1 \to -(p \, k)$, and $x_2 \to (p_+ \, k)$, where

$$w_t^2 = (\mathbf{p} - \mathbf{p}_+)^2 = -2 \, [(p \, p_+) - 1] \, . \quad (6.11)$$

It is a function of the three invariants $(p \, k)$, $(p_+ k)$, and $(p \, p_+)$. The positron spectrum $d\sigma/d\varepsilon_+$, the angular distribution $d\sigma/d\Omega_{p+}$ and the total cross

section σ_t can be calculated easily by numerical integrations of Equation (6.9).

It is obvious that the cross section for pair production in the field of a positron, differential with respect to the energy and angles of the produced electron, is identical to (6.9). On the other hand, the doubly differential cross section $d^2\sigma/d\varepsilon' \, d\Omega_{p'}$ cannot be obtained from the formula (6.9) simply by substitutions.

7. Doubly Differential Cross Section for Pair Production in the Laboratory System

Motivated by experimental investigations [27, 28] of the triplet process, Jarp and Mork [14] have calculated various cross sections in the laboratory system by numerical integrations. Some of their results can easily be reproduced with higher accuracy using the Eqs. (6.9) and (A1). In the laboratory system the initial electron is at rest, i. e. $\boldsymbol{p} = 0$, $\varepsilon = 1$, and $(p \, k) = k$. Then the doubly differential cross section has the form

$$\sigma(\varepsilon_+, \theta_+) \equiv \frac{d^2\sigma}{d\varepsilon_+ \, d(\cos \theta_+)}$$
$$= a \, r_0^2 \frac{p_+}{k} \frac{\sqrt{\varrho_t^2 - 4}}{\varrho_t} \frac{1}{\pi} \int A_t \, d\Omega_{p'} \quad (7.1)$$

where

$$\varrho_t^2 = 2 \, [k + 1 - \varepsilon_+ - k(\varepsilon_+ - p_+ \cos \theta_+)] \, . \quad (7.2)$$

θ_+ is the angle between the momenta $\boldsymbol{k}$ and $\boldsymbol{p}_+$ of the incoming photon and the produced positron, respectively. For a fixed value of θ_+ the limits of the variable ε_+ are determined by $\varrho_t^2 \geqq 4$. From Eq. (7.2) it follows in the lab system

$$\frac{k^2 - 1 - k \cos \theta_+ \sqrt{k^2 \cos^2 \theta_+ - 4 \, k}}{(k + 1)^2 - k^2 \cos^2 \theta_+} \leqq \varepsilon_+ \leqq \frac{k^2 - 1 + k \cos \theta_+ \sqrt{k^2 \cos^2 \theta_+ - 4 \, k}}{(k + 1)^2 - k^2 \cos^2 \theta_+} \, . \quad (7.3)$$

The square root in Eq. (7.3) has to be real. This condition gives the limits of $\cos \theta_+$:

$$2/\sqrt{k} \leqq \cos \theta_+ \leqq 1 . \qquad (7.4)$$

Since the threshold of the triplet process in the laboratory system is $k = 4$, the quantity $2/\sqrt{k}$ is never greater than unity. Figure 11 shows $d^2\sigma/d\varepsilon_+ \, d(\cos \theta_+)$ for $k = 5.12$, i. e. the photon energy $h\nu = 2.616$ MeV, as a function of the positron energy ε_+ for various angles θ_+. These curves are in accordance with those in Fig. 7 of Jarp and Mork [14]. The cross section is maximum at $\theta_+ = 0$ and decreases rapidly as the angle θ_+ increases. It vanishes at the limits of ε_+ corresponding to $\varrho_t^2 = 4$.
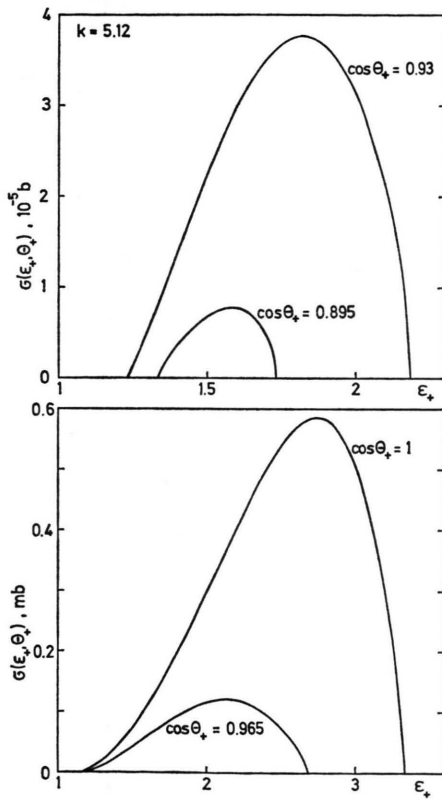

Fig. 11. Cross section $\sigma(\varepsilon_+, \theta_+)$ of triplet production in the laboratory system for the photon energy $k = 5.12$ and various angles θ_+.

8. Positron Energy Spectra and Angular Distributions in the Laboratory System

The positron spectra $d\sigma/d\varepsilon_+$ are obtained by numerical integration of the cross Sect. (7.1) over $\cos \theta_+$. For constant positron energy ε_+ the maxi-

mum angle θ_+ is determined by

$$\frac{1}{p_+}\left\{\varepsilon_+ - 1 + \frac{\varepsilon_+ + 1}{k}\right\} \leqq \cos \theta_+ \leqq 1 . \quad (8.1)$$

The limits of ε_+ are given by Eq. (7.3) setting $\cos \theta_+ = 1$.

The positron spectra for the photon energies $k = 4.4$, 5.12, 7.0, and 10.0 are plotted in Figure 12. They agree well with the corresponding curves of Jarp and Mork [14] confirming that the accuracy of their results is better than $\pm 5\%$. Experimental values [28] are available only for $k = 5.12$. Although the statistics are very poor (50 triplet events all together), the agreement between experimental and theoretical spectra is relatively good. For very high photon energies the shape of the positron spectra becomes nearly rectangular with two flat maxima, as is shown in Fig. 13 for $k = 100$.

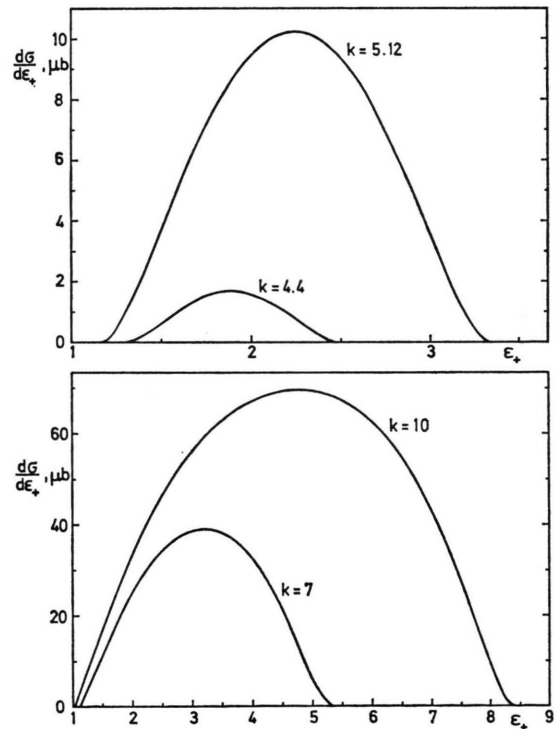Fig. 12. Triplet production in the laboratory system: positron energy spectra for various photon energies k.

The numerical integration of the cross Sect. (7.1) over ε_+ yields the angular distribution $d\sigma/d(\cos \theta_+)$ of the positrons. In Fig. 14 the results are shown in semilogarithmic plots as a function of $\cos \theta_+$ for the photon energies $k = 4.4$, 5.12, 7.0, and 10.0. As

the photon energy increases, the positrons are emitted predominantly into a more and more narrow cone in forward direction though the range allowed for the angle θ_+ [cf. Eq. (7.4)] expands. Figure 14 again verifies the results of Jarp and Mork [14]. Moreover, the angular distribution for $k = 5.12$ compares favourably with the experimental curve obtained by Augerat et al. [28].
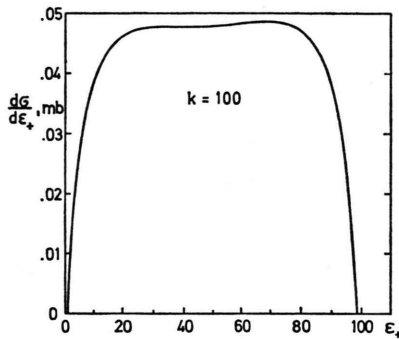

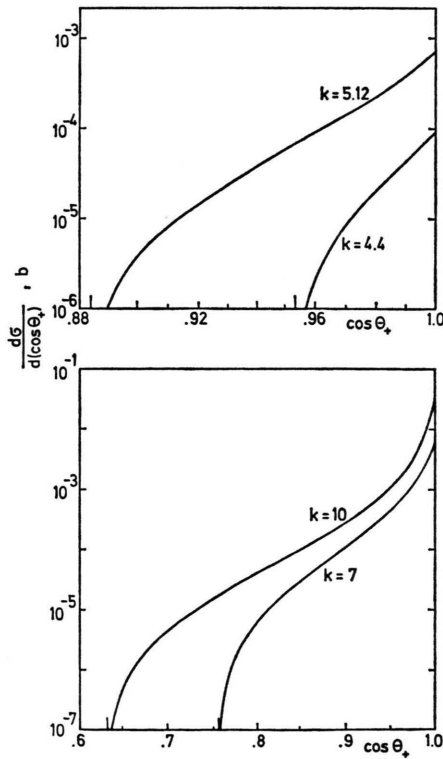Fig. 13. Triplet production in the laboratory system: positron spectrum for the photon energy $k = 100$.

Fig. 14. Angular distributions of the positrons in triplet production by photons of energies $k = 4.4$, 5.12, 7.0, and 10. The lower bounds of $\cos\theta_+$ are given by marks on the abscissae.

9. Total Cross Section for Pair Production

The total cross section σ_t for triplet production has been calculated by several authors [1, 7, 10, 11, 29, 30] using various approximations. Kopylov et al. [12] and Mork [13] applied the Monte Carlo method to integrate the differential cross section exact to lowest-order perturbation theory. However, as the photon energy increases, the accuracy of their numerical integrations becomes poor in consequence of the strong peaking effect. With the aid of the formulae (6.9) and (A1), the total cross section can easily be computed by two numerical integrations. If $\sigma(\varepsilon_+, \theta_+)$ is first integrated over the angle θ_+, the strong beaming of the positrons near forward direction is insignificant because, according to Eq. (8.1), the range of allowed angles θ_+ becomes very small at high energies k and ε_+. So the errors of the numerical integrations are negligible everywhere.

Since σ_t is a relativistic invariant, it is a function of the product $(p\,k)$ which in the laboratory system reduces to the photon energy k. The threshold is at $(p\,k) = 4$. In Table 1 the total cross section σ_t is given as a function of photon lab energy k for $4 < k \leq 5000$, compared with previous calculations (the various formulae that are available for the total triplet cross section are given by Motz et al. [31]).

It is seen that Votruba's threshold approximation [1]

$$\sigma_V = \frac{\sqrt{3}\,\pi}{972}\, \alpha\, r_0^2 (k-4)^2 \qquad (9.1)$$

is valid only very close to $k = 4$ as was pointed out by Kopylov et al. [12] and by Mork [13]. So it is of little practical use. At photon energies up to $k = 16$ there is good agreement with the results of Mork [13], σ_M, the differences being less than 1.2%.

Borsellino [10] and Ghizzetti [11] have derived an analytic expression for the total cross section neglecting the Feynman diagrams which describe exchange and the interaction of the initial electron with the incident photon ("$\gamma - e$ interaction"). Since the neglected terms have both positive and negative signs [13], they partially cancel out. Moreover, their contributions relative to the Borsellino cross section are decreasing with increasing photon energy (they are of order $1/k$ relative to the leading term [4]). So it is to be expected that the Borsellino formula is valid in the high-energy limit. In fact, this was confirmed by the calculations of Mork [13]

Table 1. Comparison of the total cross sections for triplet production as calculated in the present paper (σ_t) with the predictions of the Votruba formula (σ_V) and the Borsellino formula (σ_B), and with the numerical results of Mork (σ_M).

k	4.001	4.002	4.003	4.004	4.005	4.01	4.02	4.03	4.04	4.05
σ_t, 10^{-10} b	0.03255	0.1307	0.2951	0.5265	0.8256	3.361	13.91	32.34	59.3	95.5
σ_V, 10^{-10} b	0.03244	0.1297	0.2919	0.5190	0.811	3.244	12.97	29.19	51.9	81.1

k	4.1	4.2	4.4	4.6	5.0	5.4	5.8	6.0	6.2	6.6	7.0	7.4	7.8
σ_t, μb	0.0436	0.2133	1.110	2.940	9.85	21.22	36.80	46.0	56.1	78.7	104.0	131.5	161.0
σ_M, μb			1.1					46.2					
σ_B, μb	0.149	0.603	2.46	5.59	15.55	30.0	48.4	58.9	70.2	94.8	121.6	150.3	180.6

k	8	9	10	11	12	13	14	16	18	20	25	30
σ_t, mb	0.1764	0.2576	0.3439	0.433	0.522	0.611	0.700	0.871	1.035	1.191	1.545	1.856
σ_M, mb	0.176		0.340		0.518		0.699	0.878				
σ_B, mb	0.1962	0.278	0.363	0.451	0.538	0.625	0.711	0.877	1.037	1.188	1.534	1.838

k	35	40	45	50	60	70	80	90	100	200	300	400	500
σ_t, mb	2.131	2.376	2.598	2.800	3.154	3.459	3.726	3.963	4.176	5.58	6.40	6.98	7.42
σ_B, mb	2.108	2.350	2.569	2.769	3.121	3.425	3.691	3.928	4.140	5.55	6.38	6.96	7.40

k	600	700	800	900	1000	1500	2000	2500	3000	5000
σ_t, mb	7.78	8.09	8.35	8.58	8.78	9.56	10.11	10.53	10.88	11.83
σ_B, mb	7.76	8.07	8.33	8.56	8.77	9.55	10.10	10.53	10.87	11.83

whose results were equal to the Borsellino values σ_B at $k = 16$. A comparison with the present cross sections shows, however, that the error of σ_B does not decrease continuously above $k = 16$. Whereas σ_B is much too high near threshold, it is correct at $k \approx 18$. Then, for $35 \lesssim k \lesssim 80$, it becomes too low by about 1%. Thus the conclusion by Joseph and Rohrlich [4] that in the high-energy limit Borsellino's result represents an upper bound to the total cross section, is not quite correct. Nevertheless σ_B is a good approximation to σ_t for $k > 15$ with errors less than 1.2%.

Appendix

The integration of the fully differential cross section over the angles of the outgoing electrons results in the formula

$$
\begin{aligned}
\frac{\sqrt{\varrho^2-4}}{\pi} \int A \, d\Omega_{p_1'} = \sqrt{\varrho^2-4} &\left\{ \frac{w^2+\varrho^2}{4\,x_1 x_2}\left(\frac{x_1-x_2}{x}\right)^2 - \frac{1}{4}\left(\frac{1}{x_1}-\frac{1}{x_2}\right)^2 - \frac{\varrho^2}{2\,x^2} + \frac{2\,\varrho^2}{(w^2-4)\,x_1 x_2}\left(1+\frac{1}{w^2-4}\right) \right.\\
&+ \frac{4\,\varrho^2}{w^2(w^2-4)\,x_1{}^4}\left[3\,\frac{(w^2-2)^2}{w^2-4}\,x_1 x_2 - 2\,x^2\left\{1+\frac{6}{w^2(w^2-4)}\right\}\right] - \frac{4\,\varrho^2 x}{(w^2-4)\,x_1{}^3}\\
&+ \frac{\varrho^2}{x_1{}^2}\left[\frac{4}{w^2} - \frac{3}{2} - \frac{8}{w^2(w^2-4)^2} + \frac{(w^2-2)\,x}{w^2(w^2-4)}\right] - \frac{\varrho^2}{(w^2-4)\,x_1} + \frac{1}{R_1}\left[\frac{w^2-4\,x_2}{\varrho^2} - \frac{w^2(w^2-4)}{4\,x_1 x_2} - \frac{4}{x_1}\right.\\
&\left.+ \frac{1}{x_1{}^2}\left(w^2-\frac{w^2-2}{2}\,\varrho^2\right)\right]\right\} + \frac{L}{\sqrt{R_1}}\left\{4 + \frac{1}{x_2}\left(10-\frac{w^2}{2}\right) - \frac{2}{x_1}\,(2\,w^2 - x_2 + 4) + \frac{3\,w^2(w^2-4)}{4\,x_1 x_2}\right.\\
&+ \frac{4}{x_1 R_2}\left(x_2 - 3\,x_1 + 4 + 2\,\frac{\varrho^2-3}{x_1}\right) + \frac{w^2-4-4\,x_1 x_2/\varrho^2}{x_1 R_1}\left[\frac{w^2 R_2}{4\,x_2} - (\varrho^2-2) - 2\,x_1\right]\right\}\\
&+ \varrho\,L_1\left\{\frac{\varrho^2+2}{x^2} + \frac{8}{x_1{}^2}\right\} + \frac{L_2}{W_2}\left\{2\,\frac{w^2-2}{x_2} - \frac{\varrho^2-2-x_2}{x_1} + \frac{\varrho^2-2}{2\,x}\,(\varrho^2+x_1) + \frac{w^2-4}{R_2}\right.\\
&-2 + \frac{\varrho^2-2}{8\,x\,x_1}\,(w^2+\varrho^2-4)^2 + \frac{1}{R_2 x_1}\left[(\varrho^2-2)\left\{\left(\frac{w^2+\varrho^2}{2}-2\right)x_2 - (w^2-2)\right\} - 2\,x_2{}^2 - 4\,x_2\right]\\
&\left.+ \frac{1}{R_2 x}\left[\frac{\varrho^2-2}{2}\left\{3\,(\varrho^2-4) - w^2(\varrho^2-5)\right\} + 2\,x_1{}^2 - 6\,x_1 + (w^2-2)\,x_2\right]\right\}\\
&+ \frac{2\,\varrho\,L_3}{w\,\sqrt{w^2-4}\,x_1}\left\{4 + \frac{8\,(w^2-2)}{(w^2-4)^2} - \frac{3\,(w^2-2)}{2\,x_2} + \frac{1}{x_1}\left[x_2{}^2 - 2\,w^2 - (w^2-1)\,x_2 + \tfrac{1}{2}(w^2-2)^2\right]\right.\\
&+ \frac{\varrho^2}{2\,x}\,(\varrho^2-2) - \frac{x_2}{2\,x}\,(w^2-2) - \frac{w^2+\varrho^2-4}{4\,x\,x_2}\,(w^2-2)^2 + \frac{x}{4\,x_1 x_2}\left[(w^2-2)^2\right.\\
&\left.+ (\varrho^2-2)\,(\varrho^2-4) - 8\,\frac{\varrho^2-2}{w^2-4}\right] + \frac{4\,x^2}{w^2(w^2-4)\,x_1} - \frac{1}{R_2}\left[2\,(\varrho^2-2)\,x_2 + (w^2-4)\,x - 4\,(w^2-2)\right]\\
&+ \frac{8-\varrho^2}{2\,x_1}\,(w^2-2)\right] + \frac{1}{x\,R_2}\left[\frac{\varrho^2-2}{2}\left\{3\,(\varrho^2-4) - w^2(\varrho^2-5)\right\} - x_1(w^2-2\,x_1+4)\right]\\
&+ \frac{2}{(w^2-4)^2\,x_1}\left[w^2(w^2-2)\,(\varrho^2-4) - 2\,(\varrho^2-2) + 4\,\frac{\varrho^2}{w^2}\right] + \frac{4\,(w^2-2)\,x}{(w^2-4)\,x_1{}^2}\left[\frac{12\,x}{w^2(w^2-4)} - \frac{\varrho^2-2}{2}\right]\\
&\left.\cdot\left[1-\frac{x}{w^2 x_1}\right]\right\} - \frac{L_4}{W_4}\left\{1 + \frac{\varrho^2-2}{8\,x_1 x_2}\left[(w^2-2)^2 + (\varrho^2-2)^2 - 6\,(w^2+\varrho^2-4) + \frac{16\,x}{w^2-4}\right]\right.\\
&\left.+ \frac{2}{x_1 x_2}\,(1-x_1-x_1{}^2) + \frac{1}{w^2-4}\left(\varrho^2-4-\frac{8}{w^2-4}\right)\right\} + \{x_1 \longleftrightarrow x_2\}\,.
\end{aligned}
\tag{A1}
$$

Here

$$w^2 = (\mathbf{p}_1 + \mathbf{p}_2)^2 = 2\left[(p_1 p_2) + 1\right], \qquad \varrho^2 = (\mathbf{p}_1{}' + \mathbf{p}_2{}') = 2\left[(p_1{}' p_2{}') + 1\right],$$

$$x_1 = (k\, p_1), \quad x_2 = (k\, p_2), \qquad\qquad x = (k\, p_1) + (k\, p_2) = \frac{w^2 - \varrho^2}{2},$$

$$R_1 = \varrho^2 - 4 + 4\, x_1 + 4\,\frac{x_1{}^2}{\varrho^2}, \qquad\qquad R_2 = \varrho^2 - 4 + 2\, x_1 = w^2 - 4 \;- 2\, x_2, \qquad\qquad (\text{A2})$$

$$W_2 = \sqrt{x_2\left(\frac{\varrho^2 - 4}{4}\, x_2 + 2\,\frac{x\, x_1}{\varrho^2}\right)}, \qquad W_4 = \sqrt{(w^2 - 4)\left[\tfrac{1}{4}\,(w^2 - 4)\,(\varrho^2 - 4) + 4\,\frac{x_1 x_2}{\varrho^2}\right]},$$

$$L = \ln\left\{\frac{\varrho}{4\, x_1}\left[R_2 + \sqrt{(\varrho^2 - 4)\, R_1}\right]\right\}, \qquad L_1 = \ln\frac{\varrho + \sqrt{\varrho^2 - 4}}{2},$$

$$L_2 = \ln\left\{1 + \frac{\varrho^2}{4\, x\, x_1}\left[(\varrho^2 - 4)\, x_2 + 2\,\sqrt{\varrho^2 - 4}\; W_2\right]\right\},$$

$$L_3 = \ln\frac{(w\,\sqrt{\varrho^2 - 4} + \varrho\,\sqrt{w^2 - 4})^2}{4\,(w^2 - \varrho^2)}, \qquad L_4 = \ln\left\{1 + \frac{\varrho^2}{8\, x_1 x_2}\left[(w^2 - 4)\,(\varrho^2 - 4) \;+ 2\,\sqrt{\varrho^2 - 4}\; W_4\right]\right\}.$$

The correctness of the expression (A1) has been checked in three different ways:

(1) All terms of (A1), i.e., also those which are obtained by exchanging x_1 for x_2, have been calculated separately. Thus all the errors violating symmetry could be discovered easily.

(2) The cross sections computed with the aid of (A1) in the cms and in the laboratory system were compared with the results obtained by numerical integration of $\mathrm{d}^3\sigma/\mathrm{d}k\,\mathrm{d}\Omega_k\,\mathrm{d}\Omega_{p_1{}'}$ over $\Omega_{p_1{}'}$.

(3) In the cms the cross section $\mathrm{d}^3\sigma/\mathrm{d}k\,\mathrm{d}\Omega_k\,\mathrm{d}\Omega_{p_1{}'}$ can be integrated exactly over the azimuthal

angle of the momentum vector $\boldsymbol{p}_1{}'$ relative to the polar axis $\boldsymbol{k}$. The results calculated from this by numerical integration over the angle α between the vectors $\boldsymbol{p}_1{}'$ and $\boldsymbol{k}$ were again compared with the values of Equation (A1).

The comparisons according to (2) and (3) yielded full agreement within the accuracy of the numerical integrations in all energy regions. Since the cross section $\mathrm{d}^3\sigma/\mathrm{d}k\,\mathrm{d}\Omega_k\,\mathrm{d}\Omega_{p_1{}'}$ used agrees excellently with the results of Mack and Mitter [18], the correctness of the formula (A1) can be taken for granted.

[1] V. Votruba, Phys. Rev. **73**, 1468 [1948]; Bull. Intern. Acad. Tcheque Sci. **49**, 19 [1948].

[2] I. Hodes, Ph. D. thesis, University of Chicago, 1953 (unpublished).

[3] H. Bethe and W. Heitler, Proc. Roy. Soc. London A **146**, 83 [1934].

[4] J. Joseph and F. Rohrlich, Rev. Mod. Phys. **30**, 354 [1958].

[5] B. K. Fedyushin, Zhur. Eksp. Teor. Fiz. **22**, 140 [1952].

[6] G. M. Garibyan, Zhur. Eksp. Teor. Fiz. **24**, 617 [1953].

[7] J. A. Wheeler and W. E. Lamb, Jr., Phys. Rev. **55**, 858 [1939] and **101**, 1836 (E) [1956].

[8] V. N. Baier, V. S. Fadin, and V. A. Khoze, Soviet Phys.-JETP **24**, 760 [1967].

[9] V. N. Baier, V. S. Fadin, and V. A. Khoze, Soviet Phys.-JETP **26**, 1238 [1968].

[10] A. Borsellino, Helv. Phys. Acta **20**, 136 [1947]; Nuovo Cim. **4**, 112 [1947]; Rev. Univ. Nacl. Tucumán A **6**, 7 [1947].

[11] A. G. Ghizzetti, Rev. Univ. Nacl. Tucumán A **6**, 37 [1947].

[12] G. I. Kopylov, L. A. Kulyukina, and I. V. Polubarinov, Soviet Phys.-JETP **19**, 1158 [1964].

[13] K. J. Mork, Phys. Rev. **160**, 1065 [1967].

[14] S. Jarp and K. J. Mork, Phys. Rev. D **8**, 159 [1973].

[15] J. M. Jauch and F. Rohrlich, Theory of Photons and Electrons, Addison-Wesley Publishing Company, Inc., Cambridge 1955.

[16] Relativistic units $m\, c^2$ and $m\, c$ for energy and momentum are used. The metric is such that the product of two four-vectors $\mathbf{a} = (a_0, \boldsymbol{a})$ and $\mathbf{b} = (b_0, \boldsymbol{b})$ is defined by $(a\, b) = a_0\, b_0 - (\boldsymbol{a} \cdot \boldsymbol{b})$.

[17] T. B. Anders, thesis, Albert-Ludwig-Universität, Freiburg (Brg.) (Germany), 1961 (unpublished); Nucl. Phys. **59**, 127 [1964].

[18] D. Mack and H. Mitter, Phys. Letters **44 A**, 71 [1973].

[19] G. Elwert, Ann. Physik **34**, 178 [1939].

[20] G. Elwert and E. Haug, Phys. Rev. **183**, 90 [1969].

[21] M. S. Maxon and E. G. Corman, Phys. Rev. **163**, 156 [1967].

[22] In Eq. (23) of Ref. [9] a misprint seems to occur since this expression partly yields negative cross sections for small angles θ. By comparison with the approximate formula given earlier by the same authors [8] one may infer that the factor of L in the first bracket of $\mathrm{d}\sigma_s$ must have the form $2\,\nu + \varkappa^2/(\nu - \varkappa) - \varkappa/\varkappa_1\,(2 - \varkappa/\nu\,\varkappa_1)$. The results of the formula corrected this way are in very good agreement with the exact cross sections of the present paper thus verifying the validity of this modification.

[23] A. I. Akhiezer and V. B. Berestetskii, Quantum Electrodynamics, Interscience Publishers, Inc., New York 1965, Chapter V.

[24] In Eq. (16) of Ref. [9] the last three terms of the function g_1 seem to have the wrong sign. This can be concluded from the series expansions of g_1 given in the Eqs. (19) and (21) of BFK.

[25] G. Altarelli and F. Buccella, Nuovo Cim. 34, 1337 [1964].

[26] E. Haug, Habilitationsschrift, Eberhard-Karls-Universität, Tübingen (Germany) 1975.

[27] G. Roche, J. Arnold, J. Augerat, L. Avan, M. Avan, J. Bonnet, J. Fargeix, A. Fleury, J. Jousset, M. J. Parizet, and M. Viaille, Nucl. Instrum. Meth. 103, 533 [1972].

[28] J. Augerat, M. Avan, M. Ballet, J. Jousset, M. J. Parizet, and G. Roche, Lett. Nuovo Cim. 11, 685 [1974].

[29] K. M. Watson, Phys. Rev. 72, 1060 [1947].

[30] K. S. Suh and H. A. Bethe, Phys. Rev. 115, 672 [1959].

[31] J. W. Motz, H. A. Olsen, and H. W. Koch, Rev. Mod. Phys. 41, 581 [1969].